Friction and Molecular Deformation in the Tensile Regime

A. R. Burns, J. E. Houston, R. W. Carpick, and T. A. Michalske
Surface and Interface Sciences Department, MS 1413, Sandia National Laboratories, Albuquerque, New Mexico 87185-1413
(Received 30 July 1998)

Recent molecular level studies of energy dissipation in sliding friction have suggested a contribution from adhesive forces. In order to observe this directly, we have constructed a scanning force microscope with decoupled lateral and normal force sensors to simultaneously observe the onset of both friction and attractive forces. Measurements made on self-assembling alkanethiol films with chemically different tail groups show that friction can increase with stronger adhesive intermolecular forces and from the associated tensile deformation and collective motion of the thiol chains. [S0031-9007(99)08383-0]

PACS numbers: 61.16.Ch, 07.79.Sp, 62.20.Qp, 81.40.Pq

Studies of wearless friction at the molecular level, both experimentally and in computational simulation, have greatly advanced the understanding of this fundamental process [1,2]. It is now established that friction is proportional to the actual area of contact. Fundamental energy dissipation mechanisms include vibrational losses induced by mechanical deformations or breaking of interfacial bonds [2], as well as electronic losses to the substrate [1]. Many questions still remain as to what factors dominate, particularly when the interfacial contact is mediated by monolayers of "model lubricants" that introduce parameters such as interchain interactions, disorder, and adhesive interactions at contact. Self-assembling monolayers [3] have been used extensively as model lubricants, because they can be substantially modified in the above respects, and they are anchored firmly, relative to more fluid lubricants, to one or both contacting surfaces.

Experimental methods to examine the effects of model lubricants on the relationship between friction and load include the surface forces apparatus (SFA) [2,4] and the scanning probe atomic force microscope (AFM) [5,6]. Chemical modifications of the free tail groups that create stronger adhesive forces at the interface also result in greater friction at the contact [5]. The exact relation between friction and interfacial bonding forces is not clear, however, and is made more complicated by the occurrence of "adhesion hysteresis," where the interfacial energy measured when separating the surfaces is often greater than that obtained during the approach [4]. Moreover, both the spring-based SFA and cantilever-based AFM exhibit instabilities when making ("jump to contact") and breaking ("pull off") interfacial contacts in the common situation where the attractive force gradient exceeds the respective spring constants. Thus, friction forces are generally measured only in the repulsive regime of the contact or for a limited range in the adhesive regime during withdrawal. Finally, a typical AFM cantilever also suffers from finite mechanical coupling between the normal and lateral force sensing modes [6].

In this paper, we describe a new way of examining frictional forces over the entire adhesive interaction between a scanning probe tip and the sample surface that not only avoids the inherent mechanical instabilities of spring-based sensors, but also completely decouples normal and lateral force sensors. Frictional forces acting to dampen the tip's lateral motion are monitored independently as a function of both positive (repulsive) and negative (attractive) loads. Thus the contribution of adhesion to friction at the earliest stages of contact can be clearly characterized. Preliminary results demonstrate that chemical modification of alkanethiol tail groups to increase adhesion not only leads to significant attractive forces, but that these interactions result in a tensile deformation of the monolayer that represents another channel for energy dissipation.

The experimental method, shown schematically in Fig. 1, combines interfacial force microscopy (IFM) [7] with shear force microscopy [8,9]. IFM has been

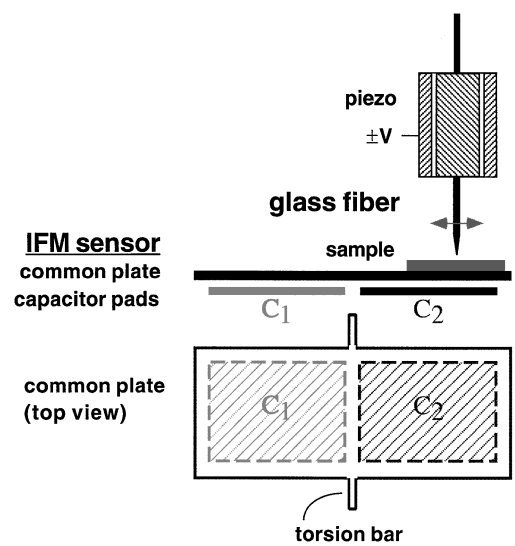

FIG. 1. Schematic of experiment. A vibrating glass fiber with a tip diameter <100 nm is brought into contact with a sample resting on an IFM sensor. The sensor measures the attractive and repulsive normal forces on the tip by maintaining an electrostatic balance of two capacitances C_1 and C_2, formed by the common plate and identical gold pads fixed on a glass substrate (not shown).

 © 1999 The American Physical Society

used previously to measure the normal adhesive forces between a stationary, single asperity tip and a substrate [10]. We now adapt an IFM sensor to measure the normal forces acting on a glass tip that is moving laterally along a substrate mounted on the sensor. Briefly, the IFM sensor [7] consists of a teeter-totter-like capacitor common plate suspended by torsion bars above two identical gold pads, creating two capacitances, C_1 and C_2 (Fig. 1). Normal forces at the end of the sensor (where the sample is located) are electrostatically balanced in a mechanically stable and noncompliant manner by application of appropriate voltages to C_1 and C_2. The sensor is mounted on a piezo (not shown) that is used for scanning and controlling the tip-sample distance. The <100 nm diameter glass tip is formed by heating and pulling the end of a 3-mm-long uncoated glass fiber that is subsequently mounted on a small piezoelectric transducer. The fiber typically has a mechanical resonance at 25–50 kHz, depending on the length, a typical Q factor of 100, and a lateral motion amplitude determined by $A_{\mathrm{piezo}}Q$, where A_{piezo} is the sinusoidal piezodrive amplitude [11]. Detection of fiber motion is accomplished by monitoring induced voltages on the drive piezo [12]. Although tip amplitudes $\ll 1$ nm can be detected, we use ~ 12 nm. Attenuation of the fiber amplitude upon interaction of the probe tip with the surface is the basis for our friction measurements. The friction force (shear force damping) is proportional to the quantity $(1 - V/V_0)$, where V is the attenuated signal at a given displacement, and V_0 is the unattenuated signal [13]. At full attenuation of the lateral motion (1.0 in Fig. 2), the shear force is equal to the driving force [13] $A_{\mathrm{piezo}}k_{\mathrm{tip}} \approx 18$ nN, where $k_{\mathrm{tip}} = 150$ nN/nm is the spring constant of the tip [14].

The substrate is a gold film on silicon upon which we adsorb densely packed, self-assembled alkanethiol monolayers, by exposure to 10^{-3} molar thiol solutions in ethanol for 24 hours [3]. We studied two thiols which have identical chain lengths, but differing tail groups. The first, $CH_3(CH_2)_{11}SH$ (hereafter called "CH_3-thiol") has a chemically inactive methyl tail group, while the second, $COOH(CH_2)_{11}SH$ (hereafter called "COOH-thiol") is terminated by a more chemically active carboxylic acid group. Although the chemistry of the bare glass tip can be modified as well, we choose here to let the native OH groups interact with the molecular monolayers. All of the experiments were conducted in a filtered, dry nitrogen atmosphere, where the relative humidity was less than 8%. Although water is expected to be present in monolayer quantities under these conditions, no capillary condensation was observed.

We show at the top of Fig. 2 the lateral "shear" damping of the tip amplitude as the oscillating fiber approaches the CH_3-thiol monolayer, together with the simultaneous normal-force response of the IFM sensor. The approach proceeds at a displacement rate of 2.5 Å/sec and is controlled by the degree of lateral damping; i.e., when it becomes greater than 80% of the undamped amplitude, the tip is withdrawn at the same rate as the approach. We estimate the displacement is accurate to within 15%, with independent piezocalibration performed against a known 50 Å feature. We have arbitrarily set zero in the displacement axis to be the point where the damping (friction) begins. The initially negative IFM sensor signal indicates a weak attractive interaction that reaches a maximum of ~ 100 nN and appears to have a total range of 7 ± 1 Å. As the tip continues the approach past approximately (-7) Å, the attractive interaction gives way to increasingly repulsive forces that elastically compress the CH_3-thiol monolayer and gold substrate. The shape of the force-displacement relation in this ~ 32 Å compressive regime is consistent with the Johnson-Kendall-Roberts (JKR) model of elastic adhesive contacts [15] discussed further below. A JKR force-displacement fit to the compression data provides an effective Young's modulus of 8 ± 1 GPa. For self-consistency, we use this value below for the friction-load relation; however, we caution that, since it was measured in the initial stages of compression, it should not be compared to stiffer values measured under much higher loads [16]. In summary, friction in the CH_3-thiol system is due first to weak attractive forces, followed by compression of the film and substrate.

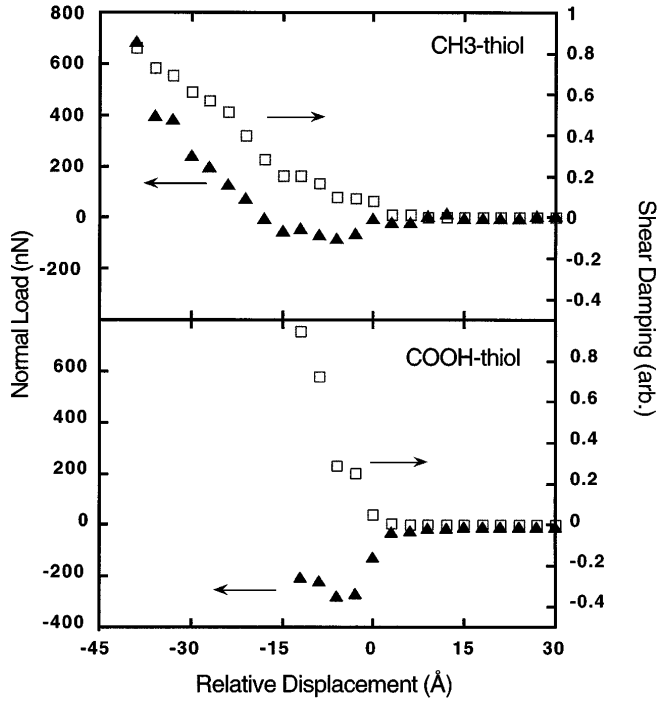

FIG. 2. Simultaneous shear damping of tip lateral motion (□) and normal forces (▲) on tip acquired for approach to CH_3-thiol monolayer (top) and to COOH-thiol monolayer (bottom). Zero displacement is arbitrarily set at the point of initial contact. It should be noted that corresponding withdrawal curves (not shown for purposes of clarity), for all the data, indicate adhesive hysteresis with stronger adhesive forces than the approach curves.

Under identical conditions and approach rate, the interaction of the same tip with the COOH-thiol sample is predominantly attractive. As shown in the lower part of Fig. 2, the tip motion is completely damped over the same range of lateral forces before appreciable compression occurs. The steep rise in friction with displacement suggests that a significant fraction of COOH-thiol chains "stand up" from their usual 30° tilt [3] to meet the probe, much like hair standing on end in response to a charged object. The ~7 Å range of the tip-COOH-thiol attractive/tensile interaction is essentially the same as that observed for the CH_3-thiol, although the forces are clearly much stronger. Thus it is possible that some of the CH_3-thiol chains stand up as well, but they are unable to significantly slow the tip down because of the relatively weak attractive forces. However, by virtue of the stronger adhesive interaction and tensile stress, the COOH-thiols bring the tip to a halt through the collective motion of the chains acting as an efficient channel for vibrational energy dissipation, in addition to the losses incurred by the making and breaking of adhesive bonds. Energy dissipation has also been associated with disorder in thiol monolayers [6]; however, previous studies [17] indicate that COOH-thiol films are not disordered relative to CH_3-thiols. Long range attractive interactions have been observed previously in normal-force displacement curves [10,18], but we cannot, at this time, attribute the onset of *friction* to noncontact long range forces. Excitation of substrate phonons and electrons has been identified as noncontact dissipation channels [19]; however, they are estimated to be considerably less efficient than those lateral forces discussed here. We can account for ~3 of the ~7 Å range through the motion of the thiol chains from the initial 30° tilt to a 0° upright position. From the JKR analysis, we calculate that another 1–2 Å can be attributed to tensile deformation of the gold substrate (and glass tip). The additional ~2–3 Å could be due to surface roughness over the ±12 nm lateral motion. It should be noted that the attractive displacement range is independent of the initial free amplitude of the tip's lateral motion for free amplitudes ≤12 nm. Thus we do not attribute the attractive/tensile interaction range to a slight tilt of the tip with respect to the samples [20].

Further insights may be gained by plotting the signals from Fig. 2 in the form of shear damping (friction) versus normal load. The difference between the two thiols is readily apparent in Fig. 3. It was demonstrated by Carpick *et al.* [21] that, for an AFM elastic single-asperity contact on bare mica, the friction force F is proportional to the tip-sample contact area A through a constant shear strength τ, analogous to SFA experiments at low loads [4]. Furthermore, these experiments revealed that the contact area was described by the JKR model of elastic adhesive contacts [15]. Following this approach, we apply the JKR model to our friction versus load plots. The JKR model predicts the dependence of the tip-sample contact area A upon the applied load L. Thus, assuming

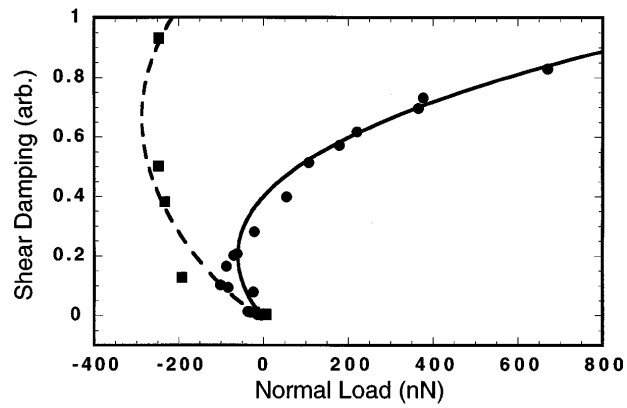

FIG. 3. Johnson-Kendall-Roberts fits to shear damping (friction) vs normal load for different monolayers: (●, solid curve) CH_3-thiol; and (■, dashed curve) COOH-thiol.

friction is proportional to the contact area, we have the relation given in Eq. (1) for a parabolic tip,

$$F = \tau A = \tau\pi\left\{\frac{R}{K}\left[L + 3\pi R\gamma + \sqrt{6\pi R\gamma L + (3\pi R\gamma)^2}\right]\right\}^{2/3}, \quad (1)$$

where R is the tip radius, and γ is the adhesion energy per unit area. The reduced modulus $K = 4/3[(1 - \nu_1^2)/E_1 + (1 - \nu_2^2)/E_2]^{-1}$ of the two materials in contact is a function of the respective Young's moduli (E_1, E_2) and Poisson ratios (ν_1, ν_2) of the tip and sample. If R and K are known, a plot of friction versus load can be used to determine both constants γ and τ. For our tip shape, determined by scanning electron microscopy to be blunt and nonparabolic, we must apply the extensions to Eq. (1) developed in Ref. [21]. As mentioned above, the JKR model also predicts the relationship between load and displacement, which yielded a value of $E_1 = 8$ GPa. If we assume $\nu_1 = 0.4$ as for most materials, and use the (E_2, ν_2) of glass [14], we obtain $K = 11$ GPa. With this value of K in the extensions to Eq. (1), we observe the JKR friction versus load fits shown in Fig. 3 for CH_3-thiol and COOH-thiol.

Averaging over many different regions of both monolayers, we obtain $\gamma = 50 \pm 21$ mJ/m^2 for the CH_3-thiol monolayer, which is in very close agreement with purely van-der-Waals-type molecular interactions [4,6,10], and $\gamma = 449 \pm 49$ mJ/m^2 for the COOH-thiol monolayer. If we subtract the 50 mJ/m^2 van der Waals contribution, the latter result is very close to the adhesive energy expected for hydrogen bonding between the CO group and OH groups on the glass tip [10] (a water monolayer, if present on the COOH-thiol, is expected to give similar results). Thus we have a reasonable explanation for the attractive intermolecular forces acting on the tip for the two thiols.

From $F = 18$ nN at 100% damping and the contact areas given by the fits [22], we obtain average values of $\tau = 13.7 \pm 1.4$ MPa and $\tau = 20.0 \pm 1.9$ MPa for CH_3-thiol and COOH-thiol, respectively. The CH_3-thiol value is similar to those obtained for hydrocarbon films in SFA experiments [4]. It is initially surprising that the difference of shear strengths for the CH_3-thiol and COOH-thiol does not correspond with the large difference in adhesion. However, the JKR fit for the CH_3-thiol includes a significant portion of positive applied loads, whereas the COOH-thiol fit has only negative loads. The absence of data in the repulsive contact regime for the COOH-thiol could mean that the JKR fit provides a lower bound to the estimated shear stress. More important is the fact that the JKR model assumes that the interfacial forces have zero spatial range [23]. Models which allow a small, finite range to these forces [24] produce curves essentially the same as those depicted in Fig. 3, and they predict that contact is first made with the surface displaced significantly upward from its equilibrium position, i.e., toward the tip, because of attractive forces. Indeed, observing finite friction with such negative loads indicates that the materials have made contact under tensile stress and thus the "range" of attractive forces should take account of film deformation as the molecules extend upward in response to the attractive forces.

In summary, we have shown that the molecular origins of friction can be examined in detail with an instrument which allows the complete adhesive interaction between a scanning probe tip and a well-defined surface to be mapped. Correlation of normal forces with lateral shear forces reveals both the attractive and repulsive nature of friction between the contacting surfaces. The purely tensile regime we measure involving the initial formation of the contact is inaccessible to an AFM because of the jump-to-contact instability. Chemical modification of the surface dramatically changes the relative contributions of attractive (adhesive) forces to friction and which may, in turn, result in additional channels of energy dissipation characterized by tensile deformation and collective chain motion. Studies such as those presented here can help reveal the contribution adhesion may have in friction and identify modes of deformation unique to molecular films.

R. W. C. acknowledges support from the Natural Sciences and Engineering Research Council of Canada. Sandia is operated by Sandia Corporation, a Lockheed Martin Company, for the United States Department of Energy under Contract No. DE-AC04-94AL85000.

[1] J. Krim, Sci. Am. **275**, No. 4, 74 (1996).
[2] B. Bhushan, J. N. Israelachvili, and U. Landman, Nature (London) **374**, 607 (1995).
[3] L. H. Dubois and R. G. Nuzzo, Annu. Rev. Phys. Chem. **43**, 437 (1992).
[4] J. N. Israelachvili, in *Handbook of Micro/Nanotribology*, edited by B. Bhushan (Chemical Rubber Co., Boca Raton, 1995), p. 267.
[5] C. D. Frisbie, L. F. Rozsnyai, A. Noy, M. S. Wrighton, and C. M. Lieber, Science **265**, 2071 (1994).
[6] R. W. Carpick and M. Salmeron, Chem. Rev. **97**, 1163 (1997).
[7] S. A. Joyce and J. E. Houston, Rev. Sci. Instrum. **62**, 710 (1991).
[8] E. Betzig, P. L. Finn, and J. S. Weiner, Appl. Phys. Lett. **60**, 2484 (1992).
[9] R. Toledo-Crow, P. C. Yang, Y. Chen, and M. Vaez-Iravani, Appl. Phys. Lett. **60**, 2957 (1992).
[10] R. C. Thomas, J. E. Houston, R. M. Crooks, T. Kim, and T. A. Michalske, J. Am. Chem. Soc. **117**, 3830 (1995).
[11] The drive amplitude is 1.23 nm/volt for our EBL 1 tube, Stavely Sensors, East Hartford, CT.
[12] J. Barentz, O. Hollricher, and O. Marti, Rev. Sci. Instrum. **67**, 1912 (1996).
[13] K. Karrai and R. D. Grober, Appl. Phys. Lett. **66**, 1842 (1995).
[14] H. Muramatsu, N. Chiba, and M. Fujihira, Appl. Phys. Lett. **71**, 2061 (1997).
[15] K. L. Johnson, K. Kendall, and A. D. Roberts, Proc. R. Soc. London A **324**, 301 (1971).
[16] S. A. Joyce, R. C. Thomas, J. E. Houston, T. A. Michalske, and R. M. Crooks, Phys. Rev. Lett. **68**, 2790 (1992).
[17] R. G. Nuzzo, L. H. Dubois, and D. L. Allara, J. Am. Chem. Soc. **112**, 558 (1990).
[18] G. S. Blackman, C. M. Mate, and M. R. Philpott, Phys. Rev. Lett. **65**, 2270 (1990).
[19] J. Krim, Comments Condens. Matter Phys. **17**, 263 (1995).
[20] M. J. Gregor, P. G. Blome, J. Schöfer, and R. G. Ulbrich, Appl. Phys. Lett. **68**, 307 (1996).
[21] R. W. Carpick, N. Agraït, D. F. Ogletree, and M. Salmeron, J. Vac. Sci. Technol. B **14**, 1289 (1996).
[22] $\sim$400 nm^2 at the minimum load. This area is smaller than the tip shape, due to small asperities and/or surface roughness.
[23] Another model, given by B. V. Derjaguin, V. M. Muller, and Y. P. Toporov, J. Colloid Interface Sci. **53**, 314 (1975), includes long range interactions; however, this model predicts zero contact area at the minimum load, which is incorrect for our data.
[24] J. A. Greenwood, Proc. R. Soc. London A **453**, 1277 (1997).